Journal of Applied Mechanics and Technical Physics, Vol. 39, No. 6, 1998

FORCES ACTING ON A COULOMB CRYSTAL OF MICROPARTICLES IN PLASMA

I. V. Schweigert and V. A. Schweigert[1]

UDC 533.9

An equilibrium two-layer structure of charged microparticles in the near-electrode layer of a radio-frequency discharge was simulated numerically using the Monte Carlo method. Depending on gas pressure, the microparticles either move chaotically or form a multilayer structure with a hexagonal lattice in a horizontal plane. Based on the experiment, a mechanism is proposed that describes the unusual structure of a plasma crystal in which particles of the lower layer are located in the vertical direction strictly under the particles of the upper layer and form vertical columns.

Introduction. The interest in the behavior of microparticles in a plasma is dictated by the important role they play in technological processes of plasma-chemical deposition and etching of films. Because of the great difference in thermal velocity between electrons and ions, the particles in a plasma acquire a negative charge Z which multiply exceeds the electron charge. The order of magnitude of the microparticle surface potential U is several electron temperatures T_e. For particles with a characteristic radius $R = 10^{-6}$–10^{-5} m and $U \sim 5$–10 eV, the surface charge is $(10^3$–$10^4)e$, where e is the elementary charge. For typical experimental conditions, therefore, the energy of the Coulomb interaction of charged particles is $U_k = e^2Z^2/a$, where a is the distance between the particles, which is significantly higher than the gas temperature T. Wigner crystallization in Coulomb systems is known to occur at $G = U_k/T \approx 135$ in the two-dimensional case and at $G \approx 170$ in the three-dimensional case [1–4]. Therefore, Ikezi [5] predicted that Coulomb crystals consisting of charged microparticles can appear in a plasma. In 1994, ordered systems of microparticles were almost simultaneously discovered in laboratory plasma by several experimental teams [6–9]. The behavior of a crystal of microparticles in a plasma is of interest, first, because they are a unique model for studying a strongly nonideal plasma and phase transitions in Coulomb systems. Second, the effects related to the interaction of crystalline (microparticles) and gaseous (electrons, ions, and neutrals) phases, the propagation of plasma waves in such systems, etc. remain poorly studied. Even the first observations of melting of a plasma crystal led to results that do not fit the commonly accepted models of Coulomb systems. The critical value of the parameter ($G \approx 20{,}000$) [8] that characterizes crystal melting in a gas-discharge plasma turned out to be significantly higher than the values typical of Coulomb systems. In a radio-frequency gas discharge burning between horizontal flat electrodes, the microparticles are "gliding" in the lower near-electrode layer, near the layer–quasineutral plasma interface. The equilibrium position of the particles is determined by the balance of oppositely directed forces (gravitational and electrical).

The shielding of the potential of the microparticles in the near-electrode layer is comparatively slight [10] and cannot be responsible for such a significant difference in the values of the parameter G. Detailed observations [11–13] conducted for different values of particle density, gas pressure, and discharge power demonstrated a number of new interesting effects. When the density is low, the particles form a one-layer hexagonal lattice which remains crystalline over the range of gas pressure and discharge power under study.

Institute of Semiconductor Physics, Siberian Division, Russian Academy of Sciences, Novosibirsk 630090. [1]Institute of Theoretical and Applied Mechanics, Siberian Division, Russian Academy of Sciences, Novosibirsk 630090. Translated from Prikladnaya Mekhanika i Tekhnicheskaya Fizika, Vol. 39, No. 6, pp. 8–15, November–December, 1998. Original article submitted January 29, 1996; revision submitted November 26, 1996.

0021-8944/98/3906-0825 $20.00

As the particle density increases, a two-layer crystal is formed owing to Coulomb repulsion, and this is in agreement with theoretical concepts [14, 15]. According to theory, however, depending on the particle density, different types of lattices with close packing (rectangular, squared, diamond-shaped, or hexagonal) should arise both in the horizontal and vertical directions [14, 15]. In experiments, however, the particles of the lower layer are located strictly under the particles of the upper layer. In a multilayer crystal, the microparticles form vertical columns. Theoretically, this type of packing of particles should not occur for a shielded potential [16]. In addition, it was experimentally observed that an increase in the gas pressure in the discharge chamber leads to an increase of the amplitude of particle oscillation around the equilibrium positions, which, ultimately, leads to crystal melting. We note that the mean kinetic energy of the particles is significantly higher than the gas temperature.

We studied an equilibrium structure of a two-layer crystal of microparticles in the near-electrode layer using numerical simulation. A mechanism that maintains the unusual vertical disposition of particles in a plasma crystal is proposed. The dependence of stability of the crystal to oscillations on the gas pressure is explained. Some results on the spatial distribution of ions in the crystal can be found in [13, 17].

Model of Ion Motion in a Crystal of Microparticles. The shielding of the microparticle potential in a plasma and the forces acting on a particle in the presence of an external electric field have been studied [18–20] using various approximations. The transfer of the momentum of ions when they are scattered on the particles induces a force that acts on the particles and is directed along the motion of ions. According to simulation results of Choi and Kushner [21], the interaction of two microparticles in a plasma is described in a first approximation by the Debye–Hückel potential. The specifics of the problem considered does not permit the use of previously obtained results to analyze the forces acting on microparticles. First, we are interested in the behavior of the particles in the near-electrode layer, where the electric-field intensity and the energy of the ions are significantly higher than in the quasineutral plasma. In addition, the mean density of ions in the layer is greater than the electron density. According to results of modeling of ion motion in the diffusion-drift approximation [15], the shielding of the particle potential in the layer is not so significant as in the quasineutral plasma. Second, to analyze the structure and stability of the crystal, it is necessary to find transverse forces that arise when the particles are shifted from their equilibrium positions rather than the force that acts in the direction of the field.

It should be emphasized that a fully self-similar analysis of the motion of the ions and microparticles that takes into account their interaction is hardly possible even on advanced supercomputers because of the substantially three-dimensional character of the problem (hexagonal symmetry of the lattice) and because of the large scatter in characteristic lengths (from micron-scale radii of the particles to centimeter-scale thicknesses of the near-electrode layers). Thus, below we study a non-self-similar formulation of the problem. The goal is to derive simple relationships for the forces acting on the particles that can be used to analyze collective effects.

We consider the motion of ions in the presence of a two-layer crystal of microparticles for experimental conditions [13] in which the behavior of microparticles in the near-electrode layer of a high-frequency discharge in helium was studied for pressures $P = 50$–200 Pa. In the plane of the layer [$\boldsymbol{\rho} = (x, y)$] particles of radius $R = 4.7$ μm formed a hexagonal lattice ($\boldsymbol{\rho}_i^1 = n_1\mathbf{a}_1 + n_2\mathbf{a}_2$, where $\mathbf{a}_1 = (a, 0)$ and $\mathbf{a}_2 = (a/2, \sqrt{3}a/2)$ are the vectors of the Bravais lattice) with a distance between the particles $a = 450$ μm. The particles of the lower layer were located at a distance $d = 0.8a = 360$ μm under the particles of the upper layer. Unless otherwise stated, the results described below refer to exactly these parameters of the lattice and a potential on the particle surface $U = 5$ eV. From the symmetry condition, it is clear that the transverse forces are equal to zero for this position of the particles. For analysis of the amplitude of the restoring force, the lower layer as a whole was shifted at a certain distance δx along the x axis relative to the upper layer.

We consider the distribution of the potential generated by the hexagonal lattice of charged particles without shielding:

$$\varphi(\mathbf{r}) = -\sum_{\boldsymbol{\rho}_1} eZ/|\mathbf{r} - \boldsymbol{\rho}_1|, \qquad \boldsymbol{\rho}_1 = n_1\mathbf{a}_1 + n_2\mathbf{a}_2.$$

In the vicinity of the particle, the potential has a Coulomb character $\varphi(\mathbf{r}) = eZ/r$. At long distances, it is convenient to use the Fourier expansion

$$\varphi(\mathbf{r}) = \sum_{\mathbf{q}} \varphi_{\mathbf{q}}(z) \exp(i\mathbf{q}\rho), \qquad \mathbf{q} = n_1\mathbf{b}_1 + n_2\mathbf{b}_2,$$

where $\mathbf{b}_1$ and $\mathbf{b}_2$ are the vectors of the reciprocal Bravais lattice. The coefficients $\varphi_{\mathbf{q}}(z)$ have the form

$$\frac{\partial^2\varphi_{\mathbf{q}}}{\partial z^2} - q^2\varphi_{\mathbf{q}} = -4\pi eZ\delta(z)/S,$$

where $S = \sqrt{3}a^2/2$ is the area of an elementary cell of the hexagonal lattice. For subsequent analysis, it is convenient to represent the potential of the layer as $\varphi(\mathbf{r}) = \varphi_0(z) + \varphi_1(\mathbf{r})$ and $\varphi_0(z) = \int \varphi(\mathbf{r})\, d\rho$, where integration is performed with respect to the transverse coordinates. The part of the potential that depends on the transverse coordinates is described by harmonics with $\mathbf{q} \neq 0$

$$\varphi_{\mathbf{q}}(z) = -\frac{4\pi eZ}{qS} \exp(-q|z|)$$

and decreases exponentially with distance z from the layer. The minimum value of the vector of the reciprocal lattice is $2\pi/a$, and φ_1 rapidly decreases for $z > z_* = a/2\pi$. For experimental conditions, $z_* \approx 70$ μm turns out to be much smaller than the characteristic values of the electron Debye length $r_d = \sqrt{T_e/4\pi e^2 n_e}$ which, for typical values of density $n_e = 10^{14}$–10^{15} m^{-3} and electron temperature $T_e = 3$–7 eV, lies within 400 to 2000 μm. Therefore, the role of electrons in the shielding of the part of the potential that depends on the transverse coordinates is insignificant. A more complicated problem of ion shielding is considered below.

In accordance with the commonly accepted model for the near-electrode layer, the longitudinal field in the layer was considered to be linearly increasing with distance from the interface between the layer and the quasineutral plasma ($z = 0$):

$$\begin{gathered} E = 4\pi\rho z, \quad 0 < z < z_1, \qquad E = E(z_1) + 4\pi\rho(z - z_1), \quad z_1 < z < z_2, \\ E = E(z_2) + 4\pi\rho(z - z_2), \quad z > z_2. \end{gathered} \tag{1}$$

Here z_1 and z_2 are the coordinates of the upper and lower layers of charged particles. The electric field in (1) includes the field of the space ion charge of constant density ρ and the field of two uniformly charged planes of microparticles. The latter is described by a potential φ_0 that corresponds to the potential of a uniformly charged layer with the density of negative charge $\rho_l = eZ/S$. Thus, we have $E(z_1) = 4\pi\rho z_1 - 4\pi\rho_l$ and $E(z_2) = 4\pi\rho z_2 - 4\pi\rho_l$. In equilibrium, the gravitational force gM that acts on the microparticles is balanced by the action of the electric field eZE. This allows us to find the values of the field intensity E_1 and E_2 at the points z_1 and z_2: $E(z_1) = E(z_2) = E_0 = gM/Z$, where g is the acceleration of gravity and M is the mass of microparticles. From the relation $E(z_2) = E(z_1) - 4\pi\rho_l + 4\pi\rho d$ and the condition $E(z_1) = E(z_2)$ we obtain the mean density of the space charge of the ions $\rho = eZ/Sd$ at the site of the crystal of microparticles. For $U = 5$ eV, the characteristic intensity of the field is $E_0 = 25$ V/cm and the ion density is $\rho = 2.6 \cdot 10^{14}$ m^{-3}. Since φ_1 rapidly decreases with distance from the layer, we are interested in a rather narrow region of the near-electrode layer for which the use of linear approximation of the field is justified.

Thus, the spatial distribution of the field is a superposition of the field (1) and the fields of the two layers $\mathbf{E}_1 = -\nabla\varphi_1(z - z_1, \rho)$ and $\mathbf{E}_2 = -\nabla\varphi_1(z - z_2, \rho)$, which depend on the transverse coordinates (ρ is the transverse coordinate). The force that acts on the particle is determined, first, by the transfer of the momentum of the ions when they fall on the particle

$$\mathbf{F}_1 = \int m_i \mathbf{v} n_i (\mathbf{v}\mathbf{n})\, dS \tag{2}$$

[m_i, $\mathbf{v}$, and n_i are the mass, velocity, and density of the ions, and $\mathbf{n}$ is the normal vector to the particle surface, and integration in (2) is performed over the particle surface], and, second, by the Coulomb interaction between

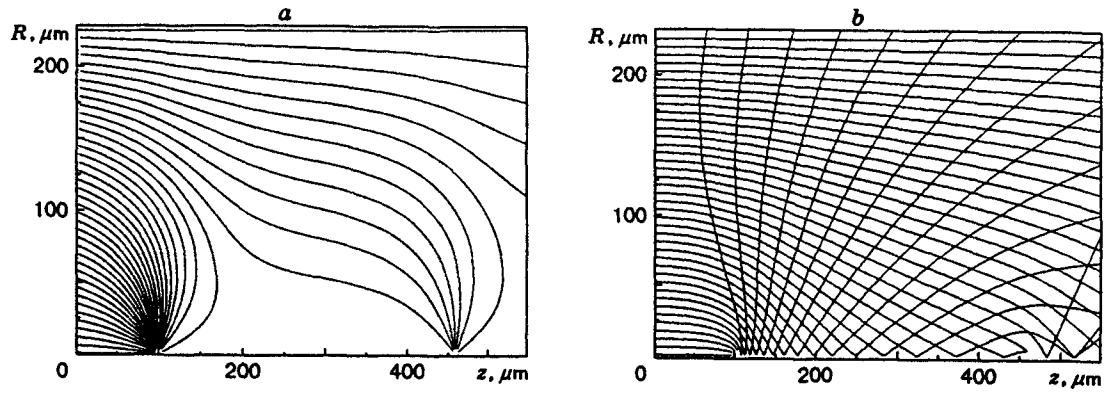

Fig. 1. Trajectories of ion motion in the drift (a) and collision-free (b) regimes ($R = \sqrt{x^2 + y^2}$).

the ions and the particle. We are interested only in transverse forces, which are defined by

$$\mathbf{F}_2^k = \int en_i(\mathbf{r})\nabla\varphi(z - z_k, \rho)\, d\mathbf{r}, \qquad k = 1, 2,$$

where k is the layer number and integration is performed over the volume of an elementary cell. The ion velocity distribution function at the upper boundary of the computational domain z_t was specified as a Boltzmann distribution function in a field $E(z_t)$. In the transverse direction, the ion density at the upper boundary n_t was constant. The lower boundary z_b of the computational domain corresponded to an absolutely absorbing electrode. In the transverse direction, the computational domain corresponded to one elementary cell of the hexagonal lattice. When the ion trajectory leaves the elementary cell, the ion is again placed in a computational domain with transverse coordinates obtained by shifting the lattice by the corresponding vector.

In Monte Carlo simulations of the ion motion, we took into account the basic process of ion scattering in helium — resonance recharging with a constant cross section. In the range of pressures studied, the mean free path of the ions λ was within 50–200 μm. Several dozens of thousands of ion trajectories were used in calculations.

Calculation Results for the Ion Motion. For an understanding of the special features of the ion motion, two limiting transfer regimes are of interest: the drift regime ($\lambda \to 0$) and the collision-free regime ($\lambda \to \infty$) (Fig. 1). For the drift transfer, the velocity of ion motion was assumed to be proportional to the local intensity of the field. For the collision-free regime, we solved Newton equations, ignoring resonance recharging. It turned out that the radial distributions of ion density behind the particles differ even qualitatively. Shaded regions with a lower ion concentration are formed behind the particles in the drift regime, whereas in the collision-free regime the ion density behind the particles increases because of the focusing action of the field of the particles. Thus, as we pass from high pressures (the drift regime) to lower pressures (the collision-free regime), we should expect the occurrence of an elevated ion-density region behind the particles.

For pressures of 50–200 Pa, an intermediate case is realized, where resonance recharging cannot be ignored and the ion velocity is not a local function of the electric-field intensity. The cross section of resonance recharging of the ions in the test gas is defined as a function of the ion energy. After a collision, the ion energy is determined by the gas temperature of the gas, and it is significantly lower than the mean energy of the ions in the near-electrode layer $e\lambda E_0$. Therefore, the attraction of the ion by the particle strongly affects the ion trajectory exactly after resonance recharging, which is manifested as an inflection. The length of the potential well for an ion can be evaluated assuming that the field in the vicinity of a particle is a superposition of the uniform external field E_0 and the Coulomb field of the particle: $\varphi(r) = -rE_0 \cos\theta - eZ/r$, where r is the distance from the particle and θ is the angle between the direction of the external field and the radius-vector. The diameter of the potential well for $\theta = \pi/2$ is equal to the distance from the particle to the edge of the well $L = \sqrt{eZ/E_0} \approx 100$ μm in the direction in which the field acts ($\theta = 0$). Most of the ions that experienced recharging in the potential well ultimately arrive at the particle. The remaining ions after recharging are

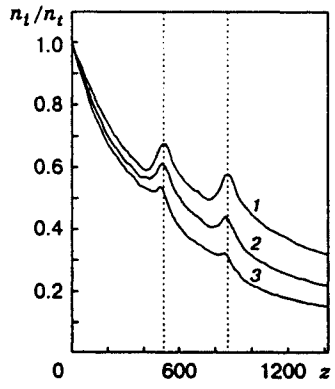

Fig. 2. Distribution of ion density averaged over the transverse coordinates for various values of the mean free path λ_i = 200, 100, and 50 μm (curves 1–3, respectively).

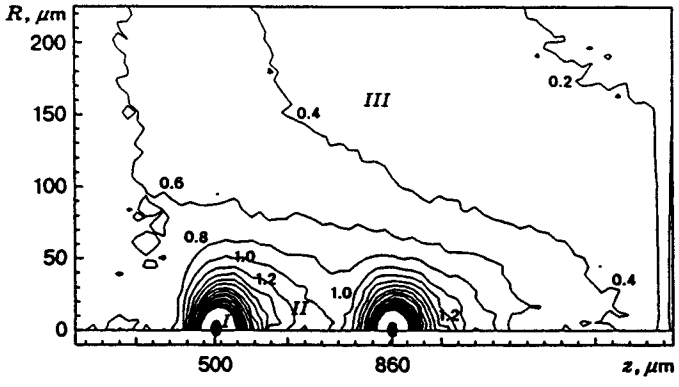

Fig. 3. Ion density distribution.

focused by the particle field. As noted above, the transverse field rapidly decreases as the distance from the layer increases. Therefore, if the next recharging occurs when $|z - z_1| > z_*$, the focused ions move already parallel to the external-field direction. The lower particles begin to affect the ion motion only at distances of the order of z_* from the ion to the lower layer.

The results obtained in ion density calculations (Figs. 2 and 3) are in good agreement with the qualitative analysis of the ion trajectories. The ion density averaged over the transverse coordinates (x, y) decreases toward the electrode because of the increase in the magnitude of the electric field and, hence, the drift velocity of the ions. The ions captured by the potential well give a maximum of the mean concentration near the particles, which is clearly seen in isolines of the ion density averaged over the azimuthal angle (Fig. 3). The ion density in the vicinity of a particle (in region I) is higher than the mean value by a factor of dozens. Behind the particles we can see a "tail" of ions, which is caused by ion focusing (region II). The ion density here is severalfold higher than the mean value. In region III of undisturbed motion, the ion concentration varied weakly in the radial direction. The distance from the upper edge of the potential well to the particle ($\sqrt{2} - 1 \approx 0.414L$) is smaller than L. That is why, probably, there are more ions behind the particle than ahead of it, and the longitudinal force component F_z is directed toward the electrode. Because of the long-range character of Coulomb interaction, the transfer of the momentum of the ions at the moment they hit the particle makes a small contribution to the total force that acts on the particle from the side of the ions. When the lower layer is shifted relative to the upper layer, the longitudinal components of the forces remain

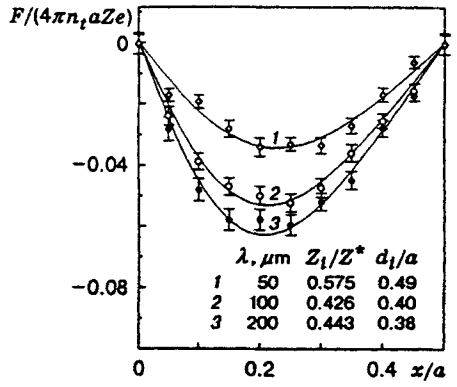

Fig. 4. Dependence of the transverse restoring force acting on the particle upon its displacement, calculated from an effective ion charge with parameters Z_i and d_i (solid curves) and using the Monte Carlo method (points): vertical bars indicate the error of statistical calculations; $\varphi = 5$ eV, $a = 450$ μm, $d = 360$ μm, $Z^* = Zn_t/\rho$.

almost constant. We note that the ions exert a weak action on the particle as compared to the gravitational force and the force of the electric field. As follows from the above analysis of the distribution of the potential of the layer, the lower particles should affect the ion motion only for $|z - z_2| \approx z_*$. This is confirmed by the calculation results for ion density distributions in various planes. Since $d \gg z_*$, the displacement of the lower layer has practically no effect on the speed of charging of the upper particles, and the transverse force for the upper particles equals zero to within the accuracy of statistical error. Although only about 15% of the ion flow are captured by the upper particles, the speed of charging of the lower particles in the case of zero displacement is higher than that of the upper particles because of the effect of ion focusing. As the displacement of the lower lattice relative to the upper lattice increases, the speed of charging of the lower particles decreases monotonically.

From the viewpoint of the analysis of the equilibrium structure of the crystal of particles, the most interesting consequence of ion focusing is a transverse restoring force that arises when the lower particles are shifted relative to the upper particles (Fig. 4). Since the problem is symmetric, the restoring force is equal to zero for $\delta x = 0$ and $a/2$. Depending on the mean-free path, the maximum of the restoring force lies at $\delta x = (0.20\text{–}0.25)a$. As the mean-free path and the potential of the particle increase, the effect of ion focusing becomes stronger and the effective positive charge behind the particles of the upper layer increases. Hence, the amplitude of the restoring force, which is determined by the interaction between the lower particles and the ion cloud behind the upper particles, also increases.

The results of Monte Carlo calculations show that the characteristics of the ion cloud such as the ion-density distribution with respect to the coordinates and the effective charge depend weakly on the displacement of the lower layer. Therefore, the restoring force can be approximated by the force of interaction between the lower particles and a certain effective ion charge Z_i located at a fixed distance $d - d_i$ behind the upper particles. The parameters Z_i and d_i were determined by the least-squares method using the dependences of the restoring force on the displacement of the lower particles that were obtained in the Monte Carlo calculation of the ion flux. We note that the empirical dependences of the restoring force describe the calculation results fairly well (to within the accuracy of statistical error) (Fig. 4). For the pressures studied, the effective charge is $Z_i = (0.44\text{–}0.58)\, Zn_t/\rho$ and the distance to the upper particle is $d - d_i = 0.51\text{–}0.62\, a$. For typical values $n_t/\rho = 2\text{–}3$ (see Fig. 2), the effective positive charge is of the same order of magnitude as the charge of the particles. For the lower particles, however, the attraction to the ion cloud is significantly stronger than the repulsion from the upper particles since $d_i > z_*$. For a more accurate calculation of the forces acting on the particle, it is necessary to take into account the effect of the ion shielding of the potential of the particles.

This work was supported by the Russian Foundation for Fundamental Research (Grant No. 96-02-19134) and by a joint grant from the Russian Foundation for Fundamental Research and the German Scientific Society (Grant No. 96-02-0241G).

REFERENCES

1. D. S. Fisher, B. I. Halperin, and R. H. Morf, "Defects in two-dimensional electron solid and implication for melting," *Phys. Rev., B*, **20**, 4692–4712 (1979).
2. R. C. Gann, S. Chakravarty, and G. V. Chester, "Monte-Carlo simulation of the classical two-dimensional one-component plasma," *Phys. Rev., B*, **20**, 326–344 (1979).
3. R. H. Morf, "Temperature dependence of the shear modulus and melting of the two-dimensional electron solid," *Phys. Rev. Lett.*, **43**, 931–935 (1979).
4. M. Baus and J. P. Hansen, "Statistical mechanics of simple Coulomb systems," *Phys. Rep.*, **59**, 2–94 (1980).
5. H. Ikezi, "Coulomb solid of small particles in plasmas," *Phys. Fluids*, **29**, 1765–1766 (1986).
6. J. H. Chu and L. I, "Coulomb lattice in a weakly ionized colloidal plasma," *Physica A*, **205**, 183–188 (1994).
7. J. H. Chu and L. I, "Direct observation of Coulomb crystal and liquids in strongly coupled rf dusty plasmas," *Phys. Rev. Lett.*, **72**, 4009–4012 (1994).
8. H. Thomas, G. E. Morfill, V. Demmel, et al., "Plasma crystal: Coulomb crystallization in a dusty plasma," *Phys. Rev. Lett.*, **73**, 652–655 (1994).
9. A. Melzer, T. Trottenberg, and A. Piel, "Experimental determination of the charge on dust particles forming Coulomb lattices," *Phys. Lett. A*, **191**, 301–308 (1994).
10. V. A. Schweigert, "Charging and shielding of microparticles in the near-electrode layer of a high-frequency gas discharge," in: Proc. XXII ICPIG, Part IV (1995), pp. 361–364.
11. T. Trottenberg, A. Melzer, and A. Piel, "Measurement of the electric charge on particulates forming Coulomb crystals in the sheath of a radiofrequency plasma," *Plasma Sources Sci. Technol.*, **4**, 450–458 (1995).
12. A. Melzer, A. Homann, and A. Piel, "Experimental investigation of the melting transition of the plasma crystal," *Phys. Rev., E*, **53**, 2757–2761 (1996).
13. A. Melzer, V. A. Schweigert, I. V. Schweigert, et al., "Structure and stability of the plasma crystal," *Phys. Rev., E*, **54**, R46–50 (1996).
14. D. H. E. Dubin, "Theory of structural phase transitions in a trapped Coulomb crystal," *Phys. Rev. Lett.*, **71**, 2753–2756 (1993).
15. V. A. Schweigert, "Structure of a crystal of microparticles in the near-electrode layer of a high-frequency gas discharge," *Pis'ma Zh. Tekh. Fiz.*, **21**, No. 10, 57–61 (1995).
16. M. O. Robbins, K. Kremer, and G. S. Grest, "Phase diagram and dynamics of Yukawa systems," *J. Chem. Phys.*, **88**, 3286–3312 (1988).
17. V. A. Schweigert, I. V. Schweigert, A. Melzer, et al., "Alignment and instability of 'dust' crystals in plasmas," *Phys. Rev., E*, **54**, 4155–4168 (1996).
18. M. D. Kilgore, J. E. Daugherty, R. K. Porteous, and D. B. Graves, "Ion drag on an isolated particulate in a low-pressure discharge," *J. Appl. Phys.*, **73**, 7195–7202 (1993).
19. J. Perrin, P. Molinas-Mata, and P. Belinger, "Ion drag and plasma-induced thermophoresis on particles in radiofrequency glow discharge," *J. Phys., D: Appl. Phys.*, **27**, 2499–2507 (1994).
20. J. P. Bouef, "Characteristics of a dusty non-linear plasma from a particle-in-cell Monte-Carlo simulation," *Phys. Rev., A*, **46**, 7910–7920 (1992).
21. S. J. Choi and M. J. Kushner, "Mutual shielding of closed spaced particles in low pressure plasmas," *J. Appl. Phys.*, **75**, 3351–3357 (1994).